

Reza Nezafat · Reza Shadmehr · Henry H. Holcomb

## Long-term adaptation to dynamics of reaching movements: a PET study

Received: 7 November 2000 / Accepted: 12 April 2001 / Published online: 7 July 2001  
© Springer-Verlag 2001

**Abstract** Positron emission tomography (PET) was used to examine changes in the cerebellum as subjects learned to make movements with their right arm while holding the handle of a robot that produced a force field. Brain images were acquired during learning and then during recall at 2 and 4 weeks. We also acquired images during a control task where the force field was not learnable and subjects did not show any improvements across sessions. During the 1st day, we observed that motor errors decreased from the control condition to the learning condition. However, regional cerebral blood flow (rCBF) in the posterior region of the right cerebellar cortex initially increased from the control condition and then gradually declined with reductions in motor error. Correspondingly, rCBF in the ipsilateral deep cerebellar nuclei (DCN) initially decreased from the control condition and then increased with reductions in motor error. If measures of rCBF mainly reflect presynaptic activity of neurons, this result predicts that DCN neurons fire with a pattern that starts high in the control task then decreases as learning proceeds. Similarly, Purkinje cells should generally have their lowest activity in the control task. This pattern is consistent with neurophysiological recordings that find that cerebellar activity during early learning of a motor task may mainly reflect changes in coactivation of muscles of the limbs, rather than a learning specific signal. By the end of the first session, motor errors had reached a minimum and no further improve-

ments were observed. However, across the weeks a region in the anterior cerebellar cortex showed gradual decreases in rCBF that could not be attributed to changes in motor performance. Because patterns of rCBF in the cortex and nuclei were highly anti-correlated, we used structural equation modeling to estimate how synaptic activity in the cerebellar cortex influenced synaptic activity in the DCN. We found a negative correlation with a strength that significantly increased during the 4 weeks. This suggests that, during long-term recall, the same input to the cerebellar cortex would produce less synaptic activity at the DCN, possibly because of reduced cerebellar cortex output to the DCN.

**Keywords** Motor learning · Memory · Cerebellum · Reaching movements · Force fields · Brain imaging

### Introduction

The inertial dynamics of the human arm dictate a complex relationship between motion of the joints and torques. In order to faithfully produce even the most simple single joint planar movements, for example, flexion of the elbow, the brain must activate not only elbow flexors, but also shoulder flexors that counter the shoulder extension torque that is produced by the acceleration of the elbow. If the activation of the shoulder flexors is delayed until the shoulder begins to extend due to the rotation of the elbow joint, the time delays in the spinal and supraspinal sensorimotor loops are too long for an effective response, resulting in oscillation. What is needed is an ability to predict that flexion of the elbow will result in shoulder extension and to proactively intervene. Stated more generally, the sensorimotor map that transforms a desired limb trajectory to motor commands needs to have access to an internal model of the dynamics of the limb.

Some movements of patients with cerebellar damage bear resemblance to a motor control system that has lost access to this internal model (Goodkin et al. 1993;

R. Nezafat · R. Shadmehr (✉)  
Laboratory for Computational Motor Control,  
Department of Biomedical Engineering,  
Johns Hopkins University, Baltimore, MD 21205, USA  
e-mail: reza@bme.jhu.edu  
Tel.: +1-410-6142458, Fax: +1-410-6149890

H.H. Holcomb  
Maryland Psychiatric Research Center, University of Maryland,  
and Department of Radiology, Johns Hopkins University,  
Baltimore, MD 21205, USA

R. Shadmehr  
Johns Hopkins School of Medicine, 419 Traylor Building,  
720 Rutland Avenue, Baltimore, MD 21205-2195, USA

Bastian et al. 1996): the ability to predict interaction torques of moving joints and to compensate for them is affected. Cerebellar damage also affects the ability of individuals to learn to modify their motor commands in the face of changing but predictable inertial dynamics (Lang and Bastian 1999): in trying to catch a ball, cerebellar patients need to feel the ball in their hand before they respond to its weight by pushing upward. In contrast, normal individuals can learn to anticipate the dynamics of the ball and program muscle activity to meet the ball at its point of impact. Similarly, in a task where subjects were instructed to make simple reaching movements while holding a robotic arm that produced a force field, work in our laboratory has found that cerebellar degeneration profoundly affected the ability to learn to compensate for the novel forces (Smith 2001). In contrast, mild to moderate stages of basal ganglia deterioration in Huntington's disease did not have any significant effects on this type of learning. Taken together, it appears that learning a novel internal model of arm dynamics may be strongly dependent on the integrity of the cerebellum.

In order to find neural correlates of learning control of arm dynamics, functional imaging techniques were recently used as subjects made reaching movements while interacting with a robotic arm that produced a force field (Shadmehr and Holcomb 1997, 1999; Krebs et al. 1998). It was found that initial learning of the task engaged the putamen and the prefrontal cortex, while its recall at 6 h later engaged regions of the premotor cortex and the posterior parietal cortex. Because of the limitations of the positron emission tomography (PET) camera, however, the field of view in all these studies excluded most of the cerebellum. The current study was undertaken with the aim of focusing on the activation changes that occur in the cerebellum coincident with learning of arm dynamics. In addition, we asked how the cerebellar activations changed over a 4-week period as the motor skill was mastered.

## Materials and methods

We studied eight normal volunteers (mean age: 30.6 years, seven males and one female, all right handed). The protocol was approved by the Johns Hopkins University Joint Committee on Clinical Investigation. All subjects signed a consent form.

### Behavioral paradigm and imaging protocol

Our intention was to design two very similar motor tasks where the dynamics of reaching movements would be altered, resulting in similar patterns of error in the naive individual. In one task, there would be a possibility to learn the patterns of dynamics with repeated movements. However, in the other task the dynamics would be unlearnable despite repeated movements. To achieve this, we asked subjects to perform reaching movement to targets while holding the handle of a 2-degree-of-freedom lightweight robot with their right arm (Shadmehr and Brashers-Krug 1997). The robot imposed forces on the hand. In the learnable case, the forces were described by a constant relationship to hand velocity:  $F = B\dot{x}$ , where  $\dot{x}$  was the velocity vector of the hand and  $B = [0, 13; -13, 0]$  N.s/m. In the unlearnable case, the force field was non-stationary as the velocity coefficient  $B$  was changed randomly with equal probability between  $B_1 = [0, 13; -13, 0]$ ,  $B_2 = [0, -13; 13,$

$0]$ , and  $B_3 = [0, 0; 0, 0]$  from target to target. In the experiment, subjects practiced on both fields but performance improved in only the learnable field. We used the random field as a control condition with which to compare brain activations within subjects across the weeks of scanning.

Targets appeared on a computer monitor facing the subject. Distance of the target was always at 10 cm from the start position, while its direction was at  $0^\circ, 45^\circ, \dots, 135^\circ$ , chosen randomly for outward movements, and then back to the center on the subsequent target, encompassing eight total directions of movement. A cursor indicated the hand's location continuously. The desired reaching time was  $500 \pm 50$  ms: if the target was reached too soon it turned red, if it was reached too late it turned blue, and if it was reached on time it "exploded" and made a pleasing sound.

Two or 3 days before the start of the experiment, subjects were introduced to the task outside the scanner. They practiced in the *null field*, a condition where the motors of the robot were disabled, for 384 targets. They then returned on the scan day and before the first scan again reached to a sequence of 200 targets in the null field.

We were interested in quantifying the neural correlates of motor skill retention over long intervals of time. Therefore, we imaged the brain as subjects learned the force field on day 1, and then retested them on the same field on days 15 and 29. The tasks performed in the PET scanner were identical on all days. On each day, subjects were scanned 6 times at 10 min apart. On the first and sixth scans, termed *random field condition*, the force field was non-stationary as it randomly switched between fields from target to target. On scans 2–5, termed *constant field condition*, the field was stationary. On average, subjects performed 110 movements during each scan. Between scans, subjects rested, except that after the third scan on each day subjects performed an additional set of 192 movements in the field to obtain further training. No information was provided to the subject regarding the nature of the force fields. The only instruction was to try to reach each target in time.

PET scans were carried out while subjects performed the task. The scans were acquired with a bolus injection of 42 mCi  $H_2O^{15}$  using GE 4096+ whole body tomography. A catheter was placed in the left cubital vein for injection of the bolus. The motor task was initiated 1 min before administration of bolus and continued for 90 s after the injection. The 90-s period after administration of bolus was used to acquire data for image reconstruction. After this 90-s period, the motor task stopped and subjects rested until the next scan (except between scans 3 and 4, where subjects practiced an additional set of 192 movements). Scans were initiated 10 min apart. Emission scans were attenuation corrected with a transmission scan performed before the first scan. The field of view of the acquired image included the entire cerebellum and parts of the brainstem, but little or no arm regions of the motor cortex. Each scan produced 15 brain slices at a resolution of  $2.0 \times 2.0$  mm in the horizontal plane and  $2.0 \times 6.5$  mm in the coronal plane. The MR scan for each subject was obtained with a  $T_1$ -weighted sequence.

The position and velocity of the robot's handle were recorded and a performance measure was calculated based on the deviation from a straight-line trajectory to each target at 250 ms into each movement. This measure was chosen because the field produces forces that are perpendicular to the direction of motion, pushing the hand away from the direction of the target. Our measure of adaptation, change in perpendicular displacement, is the extent that the subjects learn to compensate for this perturbation.

### Image subtraction analysis

The PET images were analyzed based on statistical parametric mapping (Friston et al. 1995) using SPM99 software from the Wellcome Department of Cognitive Neurology, London, implemented in Matlab 5.2c. The 18 PET scans for each subject were realigned to the first image using a six-parameter rigid-body transformation. This resulted in an aligned set of images and mean image for each subject. MR images were coregistered with the PET images and then normalized into stereotactic space (Talairach and Tournoux 1988) using a template image from the Montreal Neurological Institute. The resulting transformations were applied to the

PET images, generating images that had a voxel size of 2.00 mm in each dimension. The normalized PET images were smoothed with an isotropic gaussian filter, full-width at half-maximum set at 12 mm. The MRIs of subjects were averaged to produce an anatomical atlas. Once the transformation of the PET data was complete, statistical parametric maps (SPMs) were created. For within-day analysis, the images within each day of the experiment were used to create the SPM, each image as a new condition. For between day analyses, the average of constant field images (scans 2–5) was used as one condition and the average of the scans in the random field condition (scans 1 and 6) was used as another condition. The significant regions were identified using an intensity threshold of 80 maximum voxel value per image. The mean flow in the gray matter was normalized to 50/min. In all the paradigms the SPM was inspected for regions of activation in the cerebellum with  $z \geq 3.0$ .

### Structural equation modeling

We were interested in asking whether across the days of the experiment there were changes in the strength of functional connectivity between regions in the cerebellar cortex and nuclei that had shown learning related activity in day 1.

We followed the approach suggested by McIntosh and colleagues (McIntosh and Gonzalez-Lima 1994) and Buchel and Friston (1997). In this analysis, the first step is to select brain regions of interest (i.e., voxels) based on subtraction analysis. On day 1, subtraction analysis identified a region in the right cerebellar cortex and another region among the right cerebellar nuclei that significantly changed activations during learning. The peak voxel from each region was selected for further analysis. We then described a set of “structural equations” that allowed us to ask how the strength of functional connectivity between these two areas changed as subjects were retested on the same field on days 15 and 29.

To describe the structural equations, one assumes that activation measured at a given region of interest influences other regions of interest via a known network structure that has unknown weights of connectivity, or path strengths. The task is to find these unknown path strengths for each condition of the experiment. In our case, the network was simply a connection from a representative voxel in the cerebellar cortex to another voxel in the ipsilateral nuclei. These voxels were the peak task related voxels that were activated in the cerebellar cortex and nuclei during the first session. The network also included separate inputs to each of the cortical and nuclei voxels from other, unknown regions. To find the unknown parameters of the network, correlations between the voxels were computed across subjects for each condition separately and used to estimate the path strengths (as described below). These correlations reflected the relative influence of one region (voxel) on the variance observed in another region.

For each day and each condition (random field or constant field), a separate set of path strength parameters was estimated. We were interested in the consistency in path strengths across conditions and the change in them across days. The sign of the path strength reflected whether the influence was suppressive (in terms of rCBF changes) or facilitatory. Mathematically, the change in the path strengths signified a change in the influence of one region on the variance observed in the connected region.

The rCBF values for the two task related voxels in the cerebellar cortex and nuclei were labeled as  $c_{ijk}$  and  $n_{ijk}$ , where  $i$  was subject number,  $j$  was scan number for that condition (i.e., 2, 3, 4, 5 for constant field condition, and 1, 6 for random field condition), and  $k$  was day number. For each condition at day  $k$ , an  $8 \times 2$  matrix  $Y_k$  was constructed:

$$Y_k = \begin{bmatrix} \sum_j c_{1jk} & \sum_j n_{1jk} \\ \sum_j c_{2jk} & \sum_j n_{2jk} \\ \vdots & \vdots \\ \sum_j c_{8jk} & \sum_j n_{8jk} \end{bmatrix}$$

The structural equations described the interactions of the network shown in Fig. 4. In the equations, measurements are made from voxels in the cerebellar cortex and nuclei, and these two regions are assumed connected from the cortex to the nuclei (with no constraint on the sign of the connection). The cortex and nuclei receive other inputs that are not specifically measured but are assumed to exist. The matrix equation is written as:

$$Y_k = Y_k P_k + X_k \quad (1)$$

in which  $P_k$  is the path coefficient with elements  $p_{ij}$ , the path that connects region  $c_i$  to region  $n_j$  and represents the path strength. In our case, this is a  $2 \times 2$  matrix. Because we assume no self-recurring influence, and no connections from the nuclei to the cortex, all but one of the elements in the matrix  $P_k$  are constrained by the network’s design to be zero. The matrix  $X_k$  represents rCBF in all other regions of the brain which also influence the cerebellar cortex and nuclei but are not specifically known. Solving the equation for  $Y_k$  we have:

$$Y_k = X_k \cdot (I - P_k)^{-1}$$

in which  $I$  is the identity matrix. The task is to find  $P_k$ . The approach is based on an analysis of the covariance between activity in two regions from which rCBF is measured. In structural equation modeling, one does not minimize a function that assigns a cost to the difference between the observed and modeled values of  $Y_k$ . Rather, one minimizes a function that assigns a cost to the difference between covariance of the measured variables, called observed covariance, and the covariance predicted by the model structure and its parameter  $P_k$ , called implied covariance.

The observed covariance is a matrix of the column zero-averaged  $Y_k$ , and is defined as:

$$S_k = \frac{1}{n-1} Y_k^T Y_k \quad (2)$$

in which  $n=2$  is the number of regions to be analyzed. The implied covariance matrix that results based on the model’s design is:

$$\Sigma_k = (I - P_k)^{-T} Z_k \cdot (I - P_k)^{-1} \quad (3)$$

in which  $Z_k = X_k^T X_k$  is the variance-covariance matrix of our residual influences. Here we assume no interaction between these residual influences, and therefore no non-zero off-diagonal elements in  $Z_k$ .

$P_k$  and  $Z_k$  will be solved for by optimizing a cost function. Typically, a maximum likelihood cost function is employed (McIntosh and Gonzalez-Lima 1994):

$$F_k = \log |\Sigma_k| + \text{tr}(S_k \Sigma_k^{-1}) - \log |S_k|_k - q \quad (4)$$

in which  $\text{tr}()$  is the trace of the matrix and  $q$  is the number of free parameters in  $P$ . If our structural model is perfect, then  $F_k$  will be zero. We wish to find the value of  $P_k$  that minimizes this function. Here we used Matlab and a gradient descent optimization method to minimize this function.

### Model verification

Having specified the model and estimated coefficients  $P_k$  for each condition, we then assessed the adequacy of the estimated model. The idea is to quantify the likelihood of the covariance matrix  $S$  to appear for a randomly selected population having covariance matrix  $\Sigma$ . It has been shown that the minimum of the maximum likelihood cost function times the number of observations minus one follows a chi-squared distribution with  $m/2 (m+1) - n$  degrees of freedom, where  $m$  is the number of observed variables and  $n$  is the number of free parameters (Bollen 1989). The null hypothesis is that the proposed network is not able to produce the observed covariances among the measured variables. To reject the null hypothesis, one requires a non-significant chi-squared value. Unfortunately, this is problematic because a low chi-squared value may also be due to a small sample size.

A better approach for validation of the significance of the path strength coefficients is to construct a null model and compare its

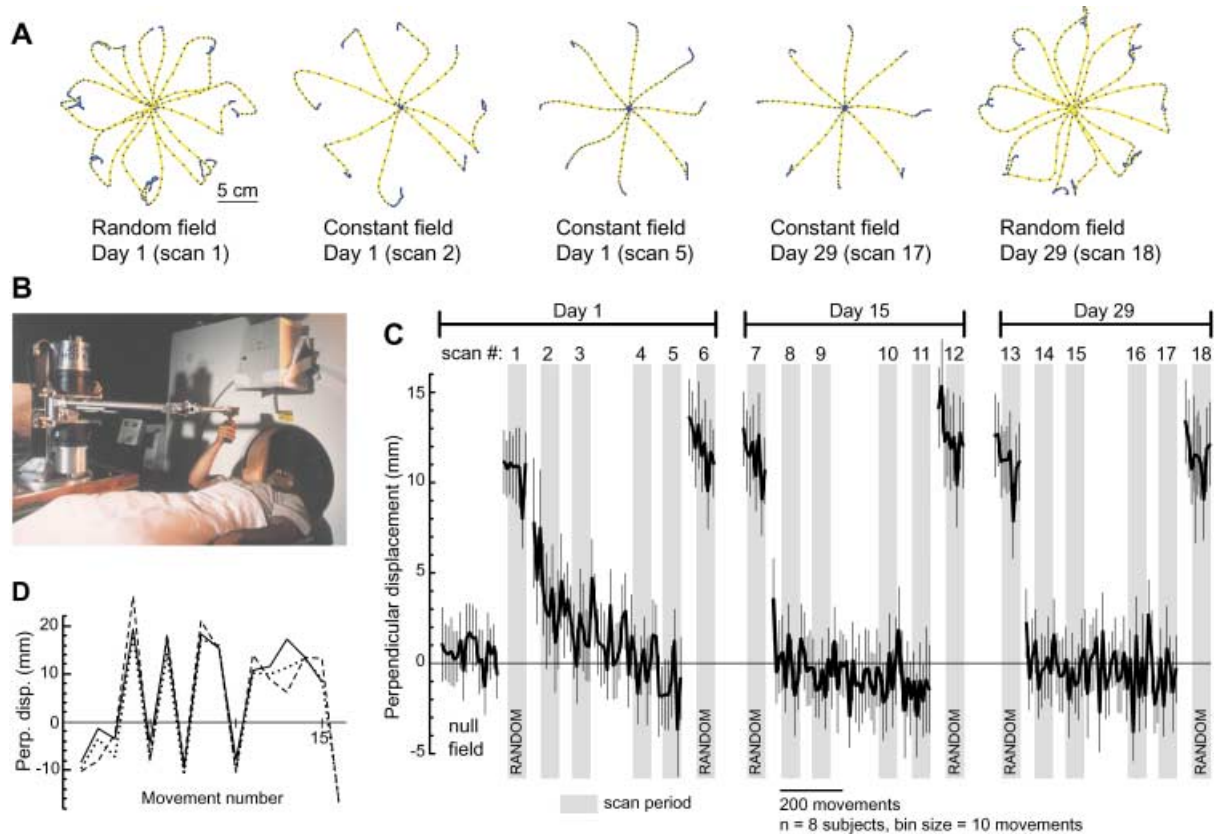


**Fig. 1A–D** Characteristics of reaching movements during the experiment. **A** Performance of a typical subject during specific scans. For each reach, a target appeared at one of eight possible directions at 10 cm from the starting position. Hand position of the subject is displayed with points at 30-ms intervals. In the random field condition, a non-stationary velocity dependent force field was imposed on the hand that significantly perturbed the hand's trajectory but was by design unlearnable. For this condition, two representative trajectories for each target are plotted. In the constant field condition, the velocity dependent force field was stationary, providing an opportunity to adapt to the field. **B** A view of the experimental setup in the scanner. **C** Performance of all subjects (means  $\pm$  SEM) as measured by the displacement of the hand's trajectory from a straight line at 250 ms into the movement. Clockwise displacements are positive; counterclockwise displacements are negative. In the random field condition, the absolute value of the displacement is plotted. **D** Mean performance across subjects in the random field for each movement toward 90°. *Solid, dashed, and dotted lines* are measured from the last scan of days 1, 15, and 29, respectively. Performance in the random field did not change across sessions

performance with the optimized model (Bollen 1989). The null model has the same structural equations but the path strengths are not allowed to change among the different conditions. In our case, we were interested in asking whether the change in the path strength between the cerebellar cortex and the nuclei across the days of the experiment was significant. After the parameters were estimated for each condition on day 1, we constructed a null model that kept the parameters constant from day 1 to subsequent days. For each day, a goodness of fit value, expressed as  $\chi^2$ , was computed for the null model. We then looked at the difference in the  $\chi^2$  statistic between this null model and the model where variables could change between the days. The significance of the differences between the models is expressed by this difference (Bollen 1989). If the goodness of fit was significantly better when

the path strengths were allowed to vary across the days, then it was concluded that there were changes in the interregional strength of connectivity during that condition.

## Results

Our initial aim was to design a situation where in the control condition dynamics of reaching movements would be altered through imposition of a force field on the hand, but that there would be little likelihood that subjects could learn a coherent internal model of the field's forces, and therefore errors would persist despite repeated practice sessions. We found that practice in the random field resulted in large errors that persisted across sessions (Fig. 1C). In contrast, in day 1 in the constant field condition, performance of subjects began with errors comparable with that of the control condition, but improved rapidly. By the end of the last constant field scan on day 1, reaching movements were essentially straight, with a slight overcompensation for the force field (mean perpendicular displacement of  $-1.4$  mm).

On day 15, performance was again poor in the random field condition, but dramatically improved upon introduction of the constant field that subjects had practiced in during day 1. The nearly step-like change in performance from the random field condition to the constant field condition (Fig. 1C) was again observed on day 29. There were no statistically significant differences between performances of subjects during scans 4 and 5 on day 1 and all other scans during recall of the internal

**Table 1** Regions with decreasing activation during constant field condition on day 1

Side	Region	<i>x</i>	<i>y</i>	<i>z</i>	<i>t</i> value
Right	Cerebellar cortex, posterior lobe	46	-74	-54	4.79
Left	Temporal lobe, inferior temporal gyrus (BA 20)	-64	-18	-26	4.71
Left	Inferior parietal lobe (BA 39)	-46	-80	24	4.56
Left	Temporal lobe, medial temporal gyrus (BA 21)	-40	2	-30	4.13

**Table 2** Regions with increasing activation during constant field condition on day 1

Side	Region	<i>x</i>	<i>y</i>	<i>z</i>	<i>t</i> value
Right	Prefrontal cortex (BA 9)	40	6	34	4.14
Right	Prefrontal cortex (BA 11)	26	20	-8	4.05
Right	Cerebellar deep nuclei	22	-54	-44	3.88
Left	Prefrontal cortex (BA 10)	14	60	-4	3.84
Left	Cerebellar deep nuclei	-14	-52	-38	3.41

model on days 15 and 29. Therefore, once the internal model was learned on day 1, it was available for recall on subsequent probes.

In the random field, forces were present during each reach but the mapping from limb trajectory to forces was not stationary from one movement to the next. Therefore, the forces could not be predicted. Not surprisingly, errors persisted and performance was unchanged across the days of the experiment (Fig. 1D).

We then examined the neural correlates of the decrease in movement errors that occurred during the constant field condition in day 1. Using a contrast that used only the images acquired during the constant field condition (i.e., non-zero contrast values for scans 2–5, and zero contrast values for scans 1 and 6), we looked for regions where blood flow correlated with the decline in error. The most significant correlations were for a region in the right posterior cerebellar cortex (Table 1). The SPM for this region and its rCBF during all the scans is shown in Fig. 2A. Interestingly, the rCBF in this region showed an increase in the first constant field scan with respect to the initial control condition ( $P < 0.01$ ), and then a decrease. This is in contrast to the general decline observed in the motor error from scan 1 to 6.

Given that the output of the cerebellar cortex is only via Purkinje neurons that inhibit the neurons in the deep cerebellar nuclei (DCN), we next looked for regions where rCBF demonstrated a gradual increase during the constant field condition (Table 2). We found that coincident with the decline in the activation of the right cerebellar cortex was an increase in the activation of regions in the right DCN (Fig. 2B), as well as in the left DCN (Table 2). Though the contrast did not explicitly look for the following behavior, we nevertheless found that rCBF in the right DCN followed the inverse of the pattern that we had observed in the cerebellar cortex from the control condition to the constant field condition. Despite the fact

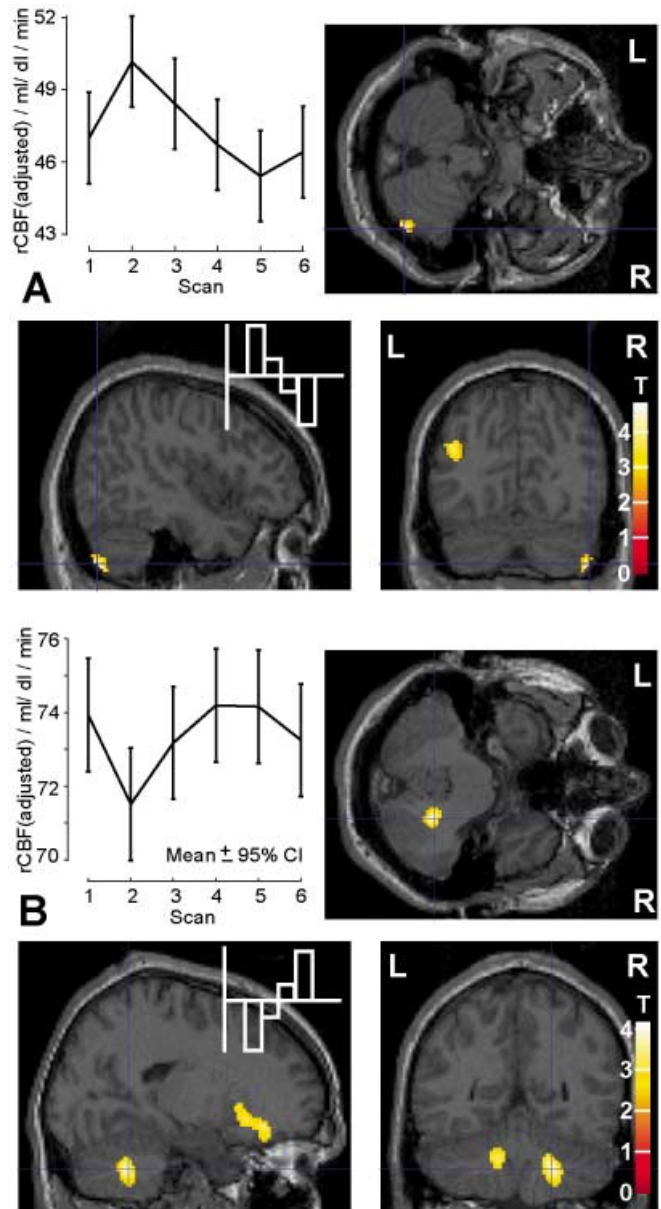


**Fig. 2A, B** Changes during acquisition of the internal model on day 1. The contrast vector used for the analysis is shown in each subfigure. The vector has non-zero values only during the constant field condition (scans 2–5). The first and sixth scans were in the random field and had a contrast of zero. **A** Regions that showed decreased rCBFs during the constant field condition. The region with the most significant change was in the right posterior cerebellar cortex (46, -74, -54,  $t=4.17$ ). The means  $\pm$  95% confidence intervals for the rCBFs at this voxel are shown. A region in the left inferior parietal lobe (-46, -80, 24,  $t=4.56$ , BA 39) is also highlighted. **B** Regions that showed increased activations during the constant field condition. A region in the right deep cerebellar nuclei (22, -54, -44,  $t=3.88$ ) is highlighted, and rCBFs at this voxel are shown. Regions among the left deep cerebellar nuclei (-14, -52, -38,  $t=3.41$ ) and in the right frontal medial gyrus (26, 20, -8,  $t=4.05$ , BA 11) are also highlighted

that error decreased from control to the constant field condition, rCBF in the cerebellar cortex initially increased while there was an initial decrease in the DCN.

We next looked for neural correlates of recall of the acquired motor skill on days 15 and 29. In general, across session comparisons are difficult because of non-task related factors that might influence metabolic activity of the brain as a function of time (Rajah et al. 1998). We assumed that any non-specific factors should be common to both the control and constant field conditions, and therefore used a time-by-condition interaction, that is, a difference between (constant field–control field) on day 1 and (constant field–control field) on a subsequent day to quantify between day changes.

A second concern was that the amount of movement error experienced by subjects was significantly higher in the early, constant field scans of day 1 vs similar scans on subsequent days. The errors were not significantly different, however, between the later scans (4, 5) of day 1 and the scans during the constant field condition (scans 2, 3, 4, 5) in days 15 and 29. Therefore, we looked for time-by-condition interactions between control and constant field scans that had comparable motor error.

In comparing days 1 and 15, we found no region in the brain that had a significant decrease in its activation. However, between day 1 and 29 we found that there was a single region with a significant decrease and it was located in the right cerebellar cortex (16, -62, -24,  $T=3.74$ ). The rCBF values for this region are plotted with respect to the control scans for each day in Fig. 3. Activation in this region of the cerebellar cortex appeared to have an orderly decline from the first day to the last, despite the fact that there was little or no difference in task performance during the scan periods.

In comparing days 1 and 15, the only region with a significant increase was in the left temporal lobe, medial gyrus, Brodmann’s area 22 (-54, -2, -22,  $T=3.59$ ). The same general area of the brain was also significantly more active in day 29 in comparison to day 1 (-50, 0, -14,  $T=3.55$ ).

We next inquired about the changes that occurred within days to the regions in the cerebellar cortex and nuclei that during day 1 had been identified to play a role in learning the task (i.e., the highlighted voxels shown in Fig. 2A, B). The patterns of rCBF change in day 1 in the cerebellar cortex and DCN were suggestive of a possible inhibitory link between these regions. While subtraction analysis between days had found no significant change in the activations of these regions, we thought that initial learning might differ from subsequent recall in the strength of functional connectivity between them.

We therefore constructed a simple network model (Fig. 4) and simulated it with linear structural equations. The model included a representation of the rCBFs in the cerebellar cortex (voxels 46, -74, -54) and DCN (voxels 22, -54, -44), as well as residual input from other, unknown regions of the brain. The task was to estimate the path strength between these two voxels for each condition in each day. From the voxel values recorded in each sub-

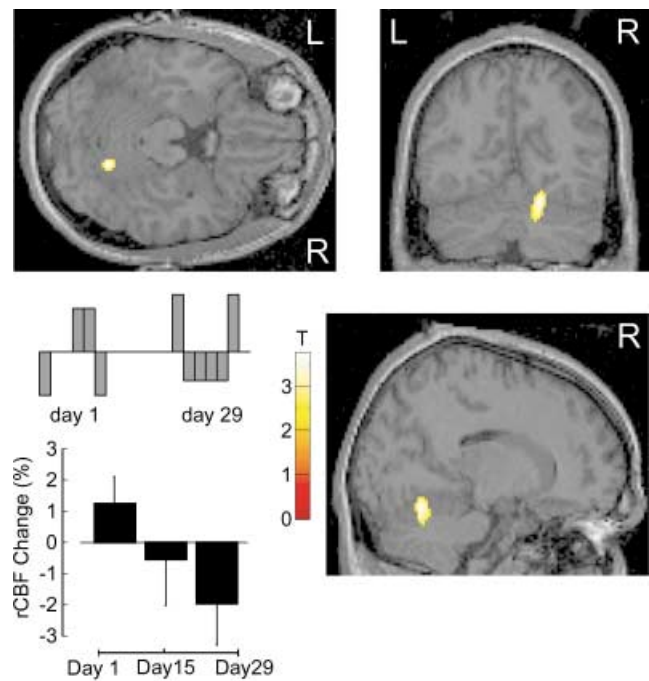


**Fig. 3** Between session (day 1 and day 29) decreases in rCBF. In order to compare scans between days, we only considered periods during which performance was similar. This eliminated the first two scans during the constant field condition on day 1. In day 1, the contrast vector had non-zero values for the random field, and the late scans of the constant field only. This was compared with the random and constant field scans on day 29. We assumed that any non-specific factors should be common to both the random and constant field conditions on each day, and therefore a difference between the two should reflect between day changes. *The highlighted region* is in the right anterior cerebellar cortex (16, -62, -24,  $T=3.74$ ). For each day, the rCBF values for this voxel are plotted during the constant field condition with respect to values for the random condition

ject a matrix  $Y_k$ , as described in “Materials and methods,” was constructed for each day  $k$ . We made a separate matrix  $Y_k$  for each condition in the task for each day, i.e., the random field condition and the constant field condition. To find the unknown parameters of the network, correlations between the two voxels were computed and a maximum likelihood cost function in Eq. 4 was minimized, resulting in an estimate of the strength of connectivity and a measure of goodness of fit in terms of  $\chi^2$ .

We found that, in all days and all conditions, the path strength between the right cerebellar cortex and right DCN was negative, reflecting a suppressive, or inhibitory-like, influence on the rCBF covariances. However, between day 1 and day 29, the strength of this inhibitory influence gradually increased (Fig. 4).

To test whether the between day connectivity changes were significant, we asked whether there would be a significant change in our cost function (Eq. 4) if we had not allowed the path strength to vary from day 1 to the subsequent days (Bollen 1989). In this approach, we defined a free model and a constrained model. For each condition, the free model allowed the path coefficient between

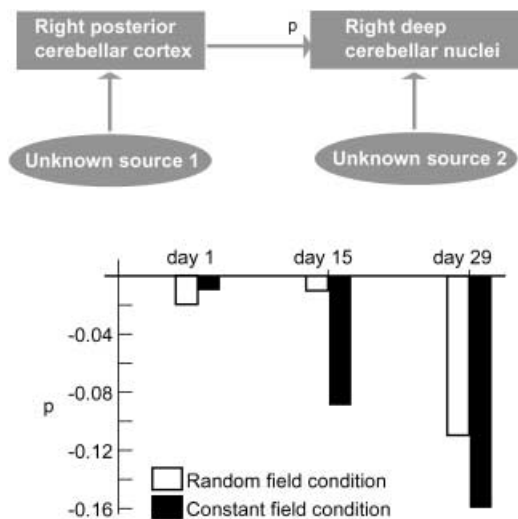


**Fig. 4** The network representing the functional connectivity between the right cerebellar cortex (voxels at 46, -74, -54) and nuclei (voxels at 22, -54, -44). The path strength was estimated from measured covariances between the two regions using structural equation modeling. The resulting values are plotted for each condition on each day of the experiment. The change in path strength during the constant field condition was found to be significant from day 1 to day 29:  $\Delta\chi^2(2)=8.181$ ,  $P<0.02$

the cerebellar cortex and nuclei to vary for each day. In the constrained model, this parameter was not allowed to change and was set to the value found for the first day's measures. The analysis then compared the goodness of fit (in terms of the change in the fit of the maximum likelihood cost function) between the free and constrained models at each day. On day 15 in the constant field condition, the change in the goodness of fit between models was not significant at  $\Delta\chi^2(2)=3.681$ ,  $P<0.2$ . However, on day 29 the improvement was significant at  $\Delta\chi^2(2)=8.181$ ,  $P<0.02$ . It is possible that in the constant field condition, between the days there was a gradual but significant increase in the magnitude of strength of connectivity between regions of right cerebellar cortex and nuclei. This increase in path strength was also observed on the last day during the random field condition: On day 29 the increase in path strength was significant at  $\chi^2(2)=7.751$ ,  $P<0.025$ .

For a second approach to verification of the model, we asked whether path strength estimation provided meaningful results if we had chosen cerebellar cortex and nuclei regions from the opposite hemisphere, contralateral to the performing arm. We chose voxels -46, -74, -54 and -22, -54, -44, which were mirror images of voxels found to be significant in the above analysis. We found that while the path strength was also always negative for this network, the change in its value from the 1st day to subsequent sessions was never significant: In the constant field condition, on day 15,  $\Delta\chi^2(2)=2.571$ ,  $P<0.5$ , and on day 29,  $\Delta\chi^2(2)=1.579$ ,  $P<0.5$ . In the random condition, on day 15,  $\Delta\chi^2(2)=0.488$ ,  $P<0.9$ , and on day 29,  $\Delta\chi^2(2)=1.345$ ,  $P<0.75$ .

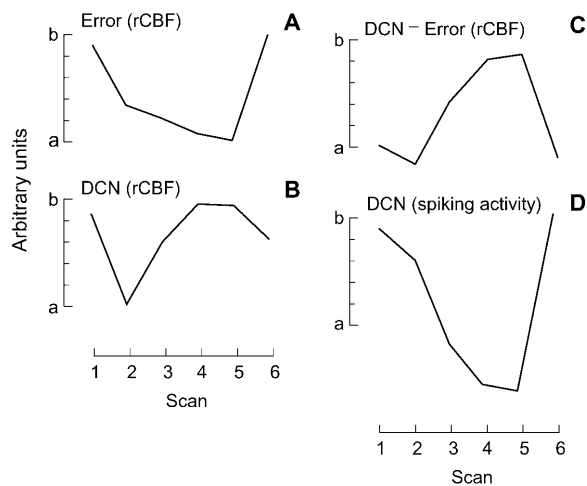


**Fig. 5A–D** Estimation of change in the firing activity of a population of task related neurons in the right DCN and Purkinje cells in the right cerebellar cortex. We assume that measured rCBF in the DCN, as shown in Fig. 2, is primarily a reflection of presynaptic activity of neurons, i.e., input to the DCN. The inputs to DCN come from three sources: precerebellar nucleus cells that give rise to mossy fibers (carrying desired state information), inferior olive neurons that give rise to climbing fibers (carrying error information), and Purkinje cells. We assume that mossy fiber input reflects a desired limb trajectory, and is constant across the scans. **A** Hypothetical change in rCBF at the DCN due to change in error. The error function is from Fig. 1. **B** Change in DCN rCBF from Fig. 2. **C** Estimate of rCBF change recorded at the right DCN due to activity of Purkinje cells. Assuming that DCN rCBF is a sum of rCBFs related to error and activity of Purkinje cells (other inputs are assumed constant), rCBF due to activity of Purkinje cells was estimated by subtracting plot A from plot B. **D** Estimate of change in firing patterns in the neurons of DCN. We assumed that neuronal activity in DCN was inhibited by activity of Purkinje cells and excited by the error signal. We further assumed that activity of inferior olive neurons was proportional to the error related rCBFs and activity of Purkinje cells was proportional to the rCBF estimated in plot C. Activity of DCN neurons was estimated by subtracting plot C from plot A

## Discussion

We studied a task where subjects learned dynamics of reaching movements. With practice, initially distorted movements became smooth, straight-line trajectories. We have hypothesized that this improvement is due to formation of an internal model in the brain. The internal model is, in part, a sensorimotor map that transforms a desired hand trajectory to forces that should be produced in order to make that movement accurately (Shadmehr and Mussa-Ivaldi 1994). We had observed that a single session of training was sufficient to allow the subject to form an accurate internal model and maintain this model for up to 5 months (Shadmehr and Brashers-Krug 1997). Research in our laboratory had also found that patients with cerebellar degeneration were profoundly impaired in acquiring the internal model, while mild to moderate basal ganglia damage in Huntington's disease spared much of this learning (Smith 2001). The current study quantified changes in cerebellar blood flow during initial learning and subsequent recall of the internal model at 2

and 4 weeks. To minimize across session artifacts that influence metabolic activity of the brain but may not be related to the recall of the motor skill, a control task was included. In this task, the field was non-stationary, effectively preventing the formation of a coherent internal model. Whereas in the initial training session in the constant field error levels gradually declined and reached a near zero level that was maintained on re-test at 2 and 4 weeks, performance in the control task displayed errors that never declined.

### Acquisition of the internal model

We found that during initial training, coincident with decreases in movement errors there were decreasing rCBFs in the right posterior cerebellar cortex and increasing rCBFs in the ipsilateral deep cerebellar nuclei (DCN). The posterior focus of the changes is reminiscent of observations made by Thach and colleagues (Martin et al. 1996) in another kind of motor learning task, prism adaptation. They reported that patients with infarcts in the distribution of the posterior inferior cerebellar artery had impaired adaptation to prism distortions but not those with lesions in the distribution of the superior cerebellar artery. Monkeys with lesions in the posterior cerebellum are also impaired in adapting to prism distortions (Baizer et al. 1999).

We found rCBFs in the right posterior cerebellar cortex and right DCN to be highly anti-correlated. In fact, activation patterns were more correlated to each other than to error changes in the task. For example, consider the scans where the condition of the task changed from random field to constant field. During this transition, while the movement errors in the task decreased, rCBFs in the cerebellar cortex tended to show an increase, and this was coincident with a decrease in the rCBFs in the DCN (Fig. 2). Similar covariations between the cortex and DCN occurred when the condition of the task changed from constant field to random field.

While it is implicit in many functional imaging papers that increases in rCBF are associated with increases in the number of action potentials in the main neurons of that region, there is good evidence that in the case of the cerebellum this assumption is false. Stimulation of climbing fibers results in complex spikes in Purkinje cells, and this is accompanied by significant increases in rCBF (Mathiesen et al. 1998). Parallel fiber stimulation also results in increased rCBFs, yet there is a net decrease in the number of simple spikes generated by Purkinje cells (Mathiesen et al. 1998). This is because parallel fiber activation provides excitatory input to inhibitory interneurons as well as dendrites of Purkinje cells. It appears that the excitation of inhibitory interneurons in the cerebellar cortex is the main contributor to rCBF increases accompanying parallel fiber stimulation (Akgoren et al. 1996). Therefore, an increase in rCBF in cerebellar cortex does not necessarily indicate increased firing in Purkinje cells. Unfortunately, because of the lo-

cal inhibitory circuitry in the cerebellar cortex, it is not apparent how one can infer Purkinje cell activity from rCBF changes.

To interpret the rCBF changes, it is important to note that changes in blood flow occur in response to changes in glucose metabolism of neurons, which in turn may be dominated by presynaptic events. Measures of rCBF with PET or functional magnetic resonance imaging (fMRI) appear to mainly reflect presynaptic activity of neurons (for review, see Jueptner and Weiller 1995). We observed that rCBF in the right DCN declined from the random to the learning condition, and then increased during learning (Fig. 2). We interpret this as a reflection of changes in the total sum of presynaptic activity in the right DCN, i.e., the change in the input to the DCN neurons.

The inputs to DCN neurons come from three main sources: precerebellar nucleus cells that give rise to mossy fibers, inferior olivary nucleus cells that give rise to climbing fibers, and Purkinje cells. If we assume that mossy fibers carry a signal related to the desired trajectory of the limb (Schweighofer et al. 1998; Wolpert et al. 1998; Spelstra et al. 2000), then it can be said that during the various conditions of the task this signal does not change. If we assume that the climbing fibers carry a signal corresponding to the errors in the task, then a measure of that signal is available in Fig. 1. The error signal is highest in the random field, then declines as the learning proceeds. If we assume that rCBF in the DCN is a simple sum of input from these three sources, then by subtracting the error signal from the DCN rCBF we arrive at an estimate of the change in presynaptic activity in the DCN due to Purkinje cell firing (Fig. 5C). Our estimate shows low levels of Purkinje cell activity during the random condition and during the initial stage of learning. This activity rises as training proceeds. Because Purkinje cells are inhibitory, their activity leads to increased rCBF in the DCN but reduced firing of DCN neurons. Assuming that DCN neuronal activity changes due to a linear combination of excitation from the error signal and inhibition from Purkinje cell activity, then the DCN neurons are estimated to fire with a pattern that starts high, then decreases as learning proceeds (Fig. 5D).

If our assumptions are reasonable, then our results suggest that DCN neuronal activity as a population is highest in the random field and during the initial stage of learning (Fig. 5D). Correspondingly, the total sum of Purkinje cell neuronal input to DCN is lowest during these conditions (Fig. 5C).

Is there any evidence for this kind of activity in the cerebellum during motor learning? To answer this question, we need to consider that muscle co-contraction in the force field learning paradigm is highest when subjects begin learning a task (and is correspondingly high in the random field), and progressively decreases as subjects learn to selectively activate muscles that counteract the field (Thoroughman and Shadmehr 1999). Studies by Smith and colleagues have demonstrated that when a task involves co-contraction of antagonist muscles, a

large majority of task related Purkinje cells decrease their firing (Frysinger et al. 1984), while neurons of the dentate and interposed nuclei increase their firing (Wetts et al. 1985). Results from Bloedel and colleagues in a study where cats learned to move a manipulandum found that magnitude of activity of dentate and interposed cells tended to decrease as the task was mastered (Milak et al. 1995). It is not known whether this is coincident with a reduction in muscle co-contractions. Therefore, our estimates of change in the rates of firing of Purkinje cells and DCN neurons, though clearly speculative, are consistent with the idea that muscle tone is expected to be highest in the random field and in the early stages of learning.

This high muscle tone results in an increased stiffness of the limb, which in turn makes the limb more resistant to perturbations imposed by the field. As the brain learns which muscles to turn on at the correct time, the need for high arm stiffness is reduced (Thoroughman and Shadmehr 1999). The framework would suggest that if the cerebellum is guiding the learning process, then while many DCN neurons should be reducing their activity as general muscle tone is reduced, a small number should be increasing their activity to reflect appropriate activation of the select muscles that counteract the field for any particular movement. Correspondingly, while many Purkinje cells would be increasing their activity as muscle tone is reduced, a small number should be decreasing their activity to reflect learning in the task. Therefore, it seems likely that metabolic costs associated with muscle-tone related changes will dominate the learning related changes during acquisition of the internal model.

#### Long-term recall of the internal model

We asked whether the rCBFs in the cerebellum showed significant changes in subsequent weeks as the internal model was recalled. We used images acquired during the random field task on each day as a control condition to account for non-specific changes between the weeks, and used a time-by-condition interaction to quantify between session changes specific to recall of the internal model. We found that there were no significant differences across the weeks in the posterior cerebellum or DCN. The contrast considered only conditions where movement errors were comparable, i.e., late stages of learning during day 1, and learning conditions during days 15 and 29. As the weeks passed, there was a significant and monotonic decrease in the rCBFs in a region of the right anterior cerebellar cortex (Fig. 3).

This suggests that some aspect of the total synaptic activity acting on the Purkinje cells in the anterior cerebellum might have declined. In models of the cerebellum where the output of the DCN reflects a force-like quantity, learning of dynamics is made possible because the appropriate excitatory synapses acting on Purkinje cells undergo a reduction in their strength, which in turn results

in the disinhibition of nuclear cells (Spoelstra et al. 2000). The evidence for this kind of mechanism is perhaps strongest in classical conditioning tasks. For example, in the models of Mauk and colleagues, improved performance is coincident with a dramatic reduction in the firing of some Purkinje cells in response to the conditioned stimulus (Medina and Mauk 1999). In models of reaching movements, the conditioned stimulus signal is replaced with a desired trajectory signal. If a reduction in synaptic strength of inputs on Purkinje cells results in reduced metabolic costs in the cerebellar cortex, then assuming that all other inputs to the cerebellar cortex are constant (for example, error related signals), the change across the weeks might be an indication of a gradual reduction in the synaptic strength of inputs upon Purkinje cells.

To better quantify the influence of time on the interactions of the cerebellar cortex and nuclei, we compared the patterns of covariance between the right posterior cerebellar cortex and the right DCN (regions which had shown task related changes during session 1) across experiment days. Functional connectivity analysis was performed using a simple network where inputs to the voxel at the DCN were assumed to be from the voxel at the right posterior cerebellar cortex, as well as potentially from other regions. The path strength from the cortex to the nuclei was estimated independently for each condition in each day of the experiment. We found a negative path strength that in a fairly orderly fashion became more negative with the passage of weeks. This suggests that a given amount of synaptic activity in the cerebellar cortex was coincident with a smaller amount of synaptic activity in the DCN.

To interpret this result, let us assume that the major source of synaptic activity in the cerebellar cortex is from climbing fibers and mossy fibers, and that, in addition to these inputs, DCN synaptic activity includes output of Purkinje cells. After the initial two scans in the constant force field, error related and state related signals did not change across the weeks. With these assumptions, the result that the same input to the posterior cerebellar cortex would produce less synaptic activity at the DCN would suggest that Purkinje cell firing activity might have been reduced across the weeks.

We tested for the significance of our result regarding the changing functional connectivity using an approach where a null model was constructed from the results obtained from the 1st day. We asked whether the errors in accounting for covariances in days 15 and 29 significantly changed if we assumed that the functional connectivity during these days was the same as that observed on day 1. The change in path strength was found to be significant by the 4th week. A second control experiment was performed by assessing the change in effective connectivity between the cerebellar cortex and DCN regions contralateral to the performing arm and mirror to the voxels on the ipsilateral side. Although the path strength was also always negative in the contralateral regions, no significant changes in connectivity were observed with

the passage of time. Therefore, it appeared that with the passage of time there was a significant increase in the magnitude of the negative path strength between regions in the right posterior cerebellar cortex and DCN.

#### Relation to earlier works

Functional imaging studies have generally found decreasing rCBFs in the cerebellum as subjects train in a motor task. When the task precluded visual feedback, repetition of finger tapping sequences (Hund-Georgiadis and von Cramon 1999) or training to move the hand in a maze while holding a pen (van Mier et al. 1998) were coincident with decreasing activations in the cerebellar cortex. When the task included visual feedback, discovery of tapping sequence with trial and error (Toni et al. 1998) was coincident with decreased activations in the cerebellar cortex while repeated practice of a given trajectory of hand movements was associated with declining activations in the dentate nucleus (Seitz et al. 1994). In a task where subjects moved a joystick that was coupled to a visual target with an altered spatial relation between the motions of the cursor and hand, training resulted in marked decreases in rCBFs in the cerebellar cortex (Flament et al. 1996). Kawato and colleagues were able to normalize for movement errors in a similar task and found significant increases in the cerebellar cortex (Imamizu et al. 2000).

As we noted above, the results of Mathiesen and colleagues (Mathiesen et al. 1998) suggest that Purkinje cell firing activity does not follow rCBF changes in the cerebellar cortex (and may in fact be opposite to these changes), even when climbing fiber activity is constant. This is because of the large rCBF cost apparently associated with synaptic activity of inhibitory neurons that convey mossy fiber information to the Purkinje cells. For this reason, we approached the problem of interpreting our rCBF results by starting from the change in the DCN.

Neuroimaging studies of long-term effects of motor practice remain rare. A prominent study (Karni et al. 1995) reported that a larger area of primary motor cortex (M1) was activated after subjects had practiced a sequential finger movement for 3 weeks. We have not observed any analogous M1 effects either during initial learning of dynamics or at 6 h (Shadmehr and Holcomb 1997, 1999). For studying internal models of motor control, however, the learning of dynamics has an important advantage over sequence learning. A quantitative and predictive model is available with which rigorous predictions about motor learning can be tested. For example, Fig. 1A shows that errors become smaller than zero. This means that, with extensive practice, subjects overcompensate the velocity-dependent force field and produce slightly S-shaped hand trajectories.

Elsewhere, we have suggested that this overcompensation results from the implementation of sensorimotor basis functions, or “primitives,” that the brain may use to

represent the internal model (Thoroughman and Shadmehr 2000). These primitives are functions that encode sensory space. In the context of this model, the problem of motor learning is to assign a weight to each primitive such that they sum to predict the dynamics necessary to compensate for the force field. After an error-based adjustment of weights during learning, the best fit to motor behavior is with primitives that encode sensory space rather coarsely, i.e., they have a broad receptive field in velocity space. These basis functions have properties that resemble the spatial fields of some Purkinje cells, which are also broadly tuned in velocity space (Coltz et al. 1999). Such broad tuning functions cause compensations to velocity-dependent force field that overestimate the forces early in movement, when velocity is low, producing S-shaped hand trajectories.

Recent neurophysiological reports show that some cells in M1 change their preferred directions of movement as a force field is learned (Li et al. 2001), and this change is similar in magnitude to the changes reported in muscle activation functions (Thoroughman and Shadmehr 1999). It is possible that a source of the changes in M1 may be from a changing input from the cerebellum. A strengthening of the functional connectivity between the cerebellar cortex and nuclei implies that, given a constant error signal, the same sensory signal representing one of the inputs to the cerebellum (for example, a desired limb trajectory) should result in an output that becomes larger and more robust with passage of time. This changing output might be one source of the observed changes in the activity of M1.

**Acknowledgements** This work was part of a Masters Thesis submitted by R.N. to the Biomedical Engineering Department at Johns Hopkins University. It was funded in part by grants from the National Institute of Neurological Disorders and Stroke (NS37422) and the William K. Warren Foundation. The work has benefited greatly from our discussions with Allan Smith and Steve Wise, and from our interactions with the scientists at the JHU Laboratory for Computational Motor Control.

#### References

- Akgoren N, Dalgaard P, Lauritzen M (1996) Cerebral blood flow increases evoked by electrical stimulation of rat cerebellar cortex: relation to excitatory synaptic activity and nitric oxide synthesis. *Brain Res* 710:204–214
- Baizer JS, Kralj-Hans I, Glickstein M (1999) Cerebellar lesions and prism adaptation in macaque monkeys. *J Neurophysiol* 81:1960–1965
- Bastian AJ, Martin TA, Keating JG, Thach WT (1996) Cerebellar ataxia: abnormal control of interaction torques across multiple joints. *J Neurophysiol* 76:492–509
- Bollen KA (1989) Structural equations with latent variables. John Wiley, Chichester
- Buchel C, Friston KJ (1997) Modulation of connectivity in visual pathways by attention: cortical interactions evaluated with structural equation modelling and fMRI. *Cereb Cortex* 7:768–778
- Coltz JD, Johnson MTV, Ebner TJ (1999) Cerebellar Purkinje cell simple spike discharge encodes movement velocity in primates during visuomotor arm tracking. *J Neurosci* 19:1782–1803

- Flament D, Ellermann JM, Kim S-G, Ugurbil K, Ebner TJ (1996) Functional magnetic resonance imaging of cerebellar activation during learning of a visuomotor dissociation task. *Hum Brain Mapp* 4:210–226
- Friston K, Holmes A, Worsley K, Poline J, Frith C, Frackowiack R (1995) Statistical parametric maps in functional imaging: a general linear approach. *Hum Brain Mapp* 2:189–210
- Frysinger RC, Bourbonnais D, Kalaska JF, Smith AM (1984) Cerebellar cortical activity during antagonist cocontraction and reciprocal inhibition of forearm muscles. *J Neurophysiol* 51:32–49
- Goodkin HP, Keating JG, Martin TA, Thach WT (1993) Preserved simple and impaired compound movement after infarction in the territory of the superior cerebellar artery. *Can J Neurol Sci* 20:S93–S104
- Hund-Georgiadis M, von Cramon DY (1999) Motor-learning-related changes in piano players and non-musicians revealed by functional magnetic-resonance signals. *Exp Brain Res* 125:417–425
- Imamizu H, Miyauchi S, Tamada T, Sasaki Y, Takino R, Putz B, Yoshioka T, Kawato M (2000) Human cerebellar activity reflecting an acquired internal model of a new tool. *Nature* 403:192–195
- Jueptner M, Weiller C (1995) Does measurement of regional cerebral blood flow reflect synaptic activity? Implications for PET and fMRI. *Neuroimage* 2:148–156
- Karni A, Meyer G, Jezard P, Adams MM, Turner R, Ungerleider LG (1995) Functional MRI evidence for adult motor cortex plasticity during motor skill learning. *Nature* 377:155–158
- Krebs HI, Brashers-Krug T, Rauch SL, Savage CR, Hogan N, Rubin RH, Fischman AJ, Alpert NM (1998) Robot-aided functional imaging: application to a motor learning study. *Hum Brain Mapp* 6:69–72
- Lang CE, Bastian AJ (1999) Cerebellar subjects show impaired adaptation of anticipatory EMG during catching. *J Neurophysiol* 82:2108–2119
- Li CSR, Padoa-Schioppa C, Bizzi E (2001) Neuronal correlates of motor performance and motor learning in the primary motor cortex of monkeys adapting to an external force field. *Neuron* 30:593–607
- Martin TA, Keating JG, Goodkin HP, Bastian AJ, Thach WT (1996) Throwing while looking through prisms. I. Focal olivocerebellar lesions impair adaptation. *Brain* 119:1183–1198
- Mathiesen C, Caesar K, Akgoren N, Lauritzen M (1998) Modification of activity-dependent increases of cerebral blood flow by excitatory synaptic activity and spikes in rat cerebellar cortex. *J Physiol* 512:555–566
- McIntosh AR, Gonzalez-Lima F (1994) Structural equation modeling and its application to network analysis in functional brain imaging. *Hum Brain Mapp* 2:2–22
- Medina JF, Mauk MD (1999) Simulations of cerebellar motor learning: computational analysis of plasticity at the mossy fiber to deep nucleus synapse. *J Neurosci* 19:7140–7151
- Milak MS, Bracha V, Bloedel JR (1995) Relationship of simultaneously recorded cerebellar nuclear neuron discharge to the acquisition of a complex, operantly conditioned forelimb movement in cats. *Exp Brain Res* 105:325–330
- Rajah MN, Hussey D, Houle S, Kapur S, McIntosh AR (1998) Task-independent effect of time on rCBF. *Neuroimage* 7:314–325
- Schweighofer N, Arbib MA, Kawato M (1998) Role of the cerebellum in reaching movements in humans: I. Distributed inverse dynamics control. *Eur J Neurosci* 10:86–94
- Seitz RJ, Canavan AG, Yaguez L, Herzog H, Tellmann L, Knorr U, Huang Y, Homberg V (1994) Successive roles of the cerebellum and premotor cortex in trajectory learning. *Neuroreport* 5:2541–2544
- Shadmehr R, Brashers-Krug T (1997) Functional stages in the formation of human long-term motor memory. *J Neurosci* 17:409–419
- Shadmehr R, Holcomb HH (1997) Neural correlates of motor memory consolidation. *Science* 277:821–825
- Shadmehr R, Holcomb HH (1999) Inhibitory control of motor memories: a PET study. *Exp Brain Res* 126:235–251
- Shadmehr R, Mussa-Ivaldi FA (1994) Adaptive representation of dynamics during learning of a motor task. *J Neurosci* 14:3208–3224
- Smith MA (2001) Error correction, the basal ganglia, and the cerebellum. PhD Thesis, The Johns Hopkins University
- Spoelstra J, Schweighofer N, Arbib MA (2000) Cerebellar learning of accurate predictive control for faster-reaching movements. *Biol Cybern* 82:321–333
- Talairach J, Tournoux P (1988) Co-planar stereotaxic atlas of the human brain. Thieme-Verlag, New York
- Thoroughman KA, Shadmehr R (1999) Electromyographic correlates of learning internal models of reaching movements. *J Neurosci* 19:8573–8588
- Thoroughman KA, Shadmehr R (2000) Learning of action through adaptive combination of motor primitives. *Nature* 407:742–747
- Toni I, Krams M, Turner R, Passingham RE (1998) The time course of changes during motor sequence learning: a whole brain fMRI study. *Neuroimage* 8:50–61
- van Mier H, Tempel LW, Perlmutter SJ, Raichle ME, Petersen SE (1998) Changes in brain activity during motor learning measured with PET: effects of hand of performance and practice. *J Neurophysiol* 80:2177–2199
- Wetts R, Kalaska JF, Smith AM (1985) Cerebellar nuclear cell activity during antagonist cocontraction and reciprocal inhibition of forearm muscles. *J Neurophysiol* 54:231–244
- Wolpert DM, Miall RC, Kawato M (1998) Internal models in the cerebellum. *Trends Cog Sci* 2:338–347